Monitoring subsurface temperature gradients using pulsed electromagnetic waves and machine learning

Pulsed ground electromagnetic waves (EM) have been deployed to scan subsurface structures by transmitting electromagnetic waves into the ground and measuring the resonant responses from different geological materials. This technology can identify various subsurface characteristics, including rock types and the presence of fluids.

For geothermal exploration, the ability to detect temperature gradients and heat sources underground is crucial. The pulsed EM technology is capable of detecting differences in rock types and the presence of fluids, which are important indicators of potential geothermal resources. In the context of finding geothermal heat, the pulsed EM technology has been trained to measure heat directly. It can aid in identifying key geological structures associated with geothermal activity, such as volcanic rocks or fault zones that might channel hot fluids. This information can be useful for inferring areas with potential geothermal activity. The technique shows great potential as a digital predrilling method for complementing direct geothermal exploration methods such as temperature gradient drilling or geothermal well logging.

We present a noninvasive method for the remote monitoring of subsurface temperature using low frequency EM pulses. Conventional ground penetrating EM [Jol, 2009] has limited applications for subsurface measurements in oil fields due to electromagnetic losses, which are rather high in the commonly used frequency range of 50 to 1000MHz, resulting in a rather shallow exploration depth.

Deeper penetration up to several kilometers has been achieved with much lower frequencies (1 − 5Mhz) using very large antennas in resistive environments such as Martian rock, ice, and permafrost [Berthelier et al., 2005, Angelopoulos et al., 2013]. We present results using the pulsed EM system [Stove and van den Doel, 2015] which emits a multispectral wave packet with significant energy in the low 1 to 5Mhz band [van den Doel et al., 2014 and Stove et al. 2023] for increased penetration depth which is in our experience sufficient to reach the comparatively shallow hot zones where steam was injected. Pulsed EM surveys were performed at 64 locations near TOWs in 3 oilfields and returns were correlated, after signal processing [Stove et al., 2018] described below, with measured down hole temperatures by training a feedforward neural network.

The results were evaluated by excluding one of the data pairs from training and use a network trained on the remaining wells to predict the excluded site, resulting in blind tests. We believe results are encouraging, though not yet fully reliable, and we discuss avenues for improvements.

1. Measurements

EM scans were performed near Temperature Observation Wells (TOWs) at three operational oilfields in California, USA, referred to here as sites A, B, and C. We obtained 21 measurements at site A, 40 measurements at site B and 3 measurements at site C.. Each site has approximately homogeneous subsurface geology, but the sites themselves differ.

Each scan consisted of the emission of a low frequency pulse and detection of returns as time domain traces recorded digitally. At each location over 100,000 traces were taken for noise reduction through stacking. A velocity model based on a calibration site was used for time to depth conversion up to 1900ft which is the largest depth for which TOW data was available.

Changes in subsurface temperature will affect conductivity and permittivity [Kummerow and Raab, 2015], which will affect the EM returns. Due to the diffuse nature of the temperature gradients, we will not see sharp reflections as in conventional subsurface imaging with GPR or seismic but more complicated effects.

Initial analysis of the data set suggested the modulation [Mather and Koch, 2011] widely used in remote sensing, as a candidate parameter to correlate with temperature. Variations in subsurface geology will also affect results and we disentangle these effects from temperature effects through machine learning.

2. Analysis

Modulation (M) and TOW temperature data (T) were down sampled to a 50ft grid and the available (M,T) pairs, except the target, were used to train a feedforward neural network to predict the target T. Once trained the neural network should extract the temperature from the EM data which contains a mix of features caused by the temperature gradients and by the geology. As the geology differs significantly between the three sites, separate networks were trained for sites A and B, referred to as the A-net and B-net. Training the network for site C is not useful as we have only 3 data pairs.

We present the measured modulation ($0 \leq M \leq 1$) derived from the EM scans and the measured TOW temperature for site A and site B, where migration from time to depth was performed using a velocity model from a calibration site.

Due to the small training set a principled approach [Goodfellow et al., 2016] using training, validation, and testing sets is not feasible and we proceeded more heuristically, experimenting with various stopping criteria for training and network architectures. Best performance was found using a 5-layer network with 3 hidden layers with 15 units, stopping training (using standard backpropagation gradient descent) at 500 iterations. Minor changes to this architecture do not affect the results very much. Small changes in results can be observed depending on the (random) initialization of the network weights, as the optimization (training) is highly non convex. To reduce this variability we have averaged results over 100 independently randomized network initializations.

The results for site A and C are depicted in Figure 1. The plots 1 to 19 represent blind tests for those specific wells, using a network trained on the other 20 wells. The last three plots, shaded green, show the result obtained by applying net-A trained on all 21 sites to predict the temperature profiles for the 3 wells of site C.

The results for site B are shown in the presentation. Each plot is a blind prediction using a network trained on the other 39 sites only.

3. Discussion

Examining the results for site A and C, we note that the results from site C (shaded green) are negative, whereas site A results are mostly qualitatively correct. This demonstrates that the modulation M is determined by geology as well as the temperature, because geology is the main difference between the sites.

Focusing on site A only, 1 to 3 are quite good, correctly identifying the steam injection location around 1300ft and the temperature curve is matched quite well, though the actual temperature is underestimated. 4 to 6 correctly identify the hot zone at the correct depth, but the steep gradient around 600ft was missed. The cold locations 7 to 9 correctly show a more or less constant low temperature, with 8 deviating most in the shallow region. Temperature profiles in 10 to 12 show a lukewarm zone around 1000ft, which shows up in 10 but not in the others. 13 to 15 follow the ground truth quite well, but ramping up a bit too slow. The hot zone in 16 to 18 appears around 100ft too deep, and maximum temperature is underestimated. TOW data for 19 to 21 is missing most of the hot zone apparently around 1500ft (deeper TOW data was not available), and the hot zone is identified around 1300ft in 19 and 21 and missed altogether in 20.

Turning to site B, we note that at some wells such as 2 and 20 we have a very good fit, at some wells like 11 and 13 the predicted hot zone has a significant depth error, and at some wells like 24 and 38 the prediction fails altogether.

The large variability in the quality of the reconstructions can be explained by local variations in geology or other subsurface anomalies. If additional data pertaining to the subsurface structure of each well were made available to the network this problem could perhaps be solved resulting in more reliable predictions.

Another approach circumventing this problem would be to use independent machine learning for each individual well for time-lapse monitoring. This would restrict use of this method near wells with a TOW, where after an initial temperature log taken in the usual way, a network is trained to correlate EM returns for that specific site, then obtain EM measurements, which is significantly cheaper than acquiring a temperature log and is non-invasive, at shorter intervals than 90 to 180 days. If changes are observed in the predicted temperature profile for a specific well this could indicate a problem and another temperature log from the TOW could be taken, potentially detecting the problem months before it would show up using the normal temperature measurement schedule.

4. Conclusions

Results presented here indicate that the modulation derived from the EM traces contains information about the subsurface temperature and could potentially be used to remotely measure temperature accurately if all other subsurface features were the same. Variation in the quality of results, in particular comparing site C reconstructions with site A reconstructions suggest the method could be improved by incorporating more information in the machine learning, in particular subsurface geology.

Another obvious source of inaccuracy is the small size of the training set which can be increased by taking more measurements. A complementary approach is to use physical simulation of the process to create simulated training data, allowing large training sets to be constructed. This approach requires accurate physical models and as electromagnetic properties of earth materials are notoriously complex, and difficult to measure in situ, this will pose challenges for further research.

It would be interesting to apply this methodology to other EM subsurface measurement methods such as resistivity surveys which should also be able to see a relation between resistivity and temperature which perhaps could be disentangled from the geological features.

References

- Angelopoulos, M. C., W. H. Pollard, and N. J. Couture, 2013, The application of ccr and gpr to characterize ground ice conditions at parsons lake, northwest territories: Cold Regions Science and Technology, 85, 22–33.
- Berthelier, J. J., S. Bonaime, V. Ciarletti, R. Clairquin, F. Dolon, A. L. Gall, D. Nevejans, R. Ney, and A. Reineix, 2005, Initial results of the Netlander imaging ground-penetrating radar operated on the Antarctic Ice Shelf: GEOPHYSICAL RESEARCH LETTERS, 32, L22305, doi:10.1029/2005GL024203.
- Goodfellow, I., Y. Bengio, and A. Courville, 2016, Deep Learning : MIT Press.
- Jol, H. M., 2009, Ground penetrating radar theory and applications: Elsevier.
- Kummerow, J., and S. Raab, 2015, Temperature Dependence of Electrical Resistivity – Part II: A New Experimental Set-up to Study Fluid-saturated Rocks: Energy Procedia, 76, 247–255.
- Mather, P. M., and M. Koch, 2011, Computer Processing of Remotely-Sensed Images: John Wiley and Sons, Ltd.
- Stove, G., G. C. Stove, and M. Robinson, 2018, New method for monitoring steam injection for Enhanced Oil Recovery (EOR) and for finding sources of geothermal heat: Presented at the

Australian Exploration Geoscience Conference.

- Stove, G., and K. van den Doel, 2015, Large depth exploration using pulsed radar: ASEG-PESA Technical Program Expanded Abstracts 2015, Perth, 1–4.
- Stove et al, 2023, Deep detection range test for a low frequency subsurface radar system (with reviewable data available online), 84th EAGE Annual Conference & Exhibition Jun 2023, Volume 2023, p.1 – 5, DOI: https://doi.org/10.3997/2214-4609.2023101348
- van den Doel, K., J. Jansen, M. Robinson, G. C. Stove, and G. D. C. Stove, 2014, Ground penetrating abilities of broadband pulsed radar in the 1-70MHz range: SEG Technical Program Expanded Abstracts 2014, Denver, 1770–1774.

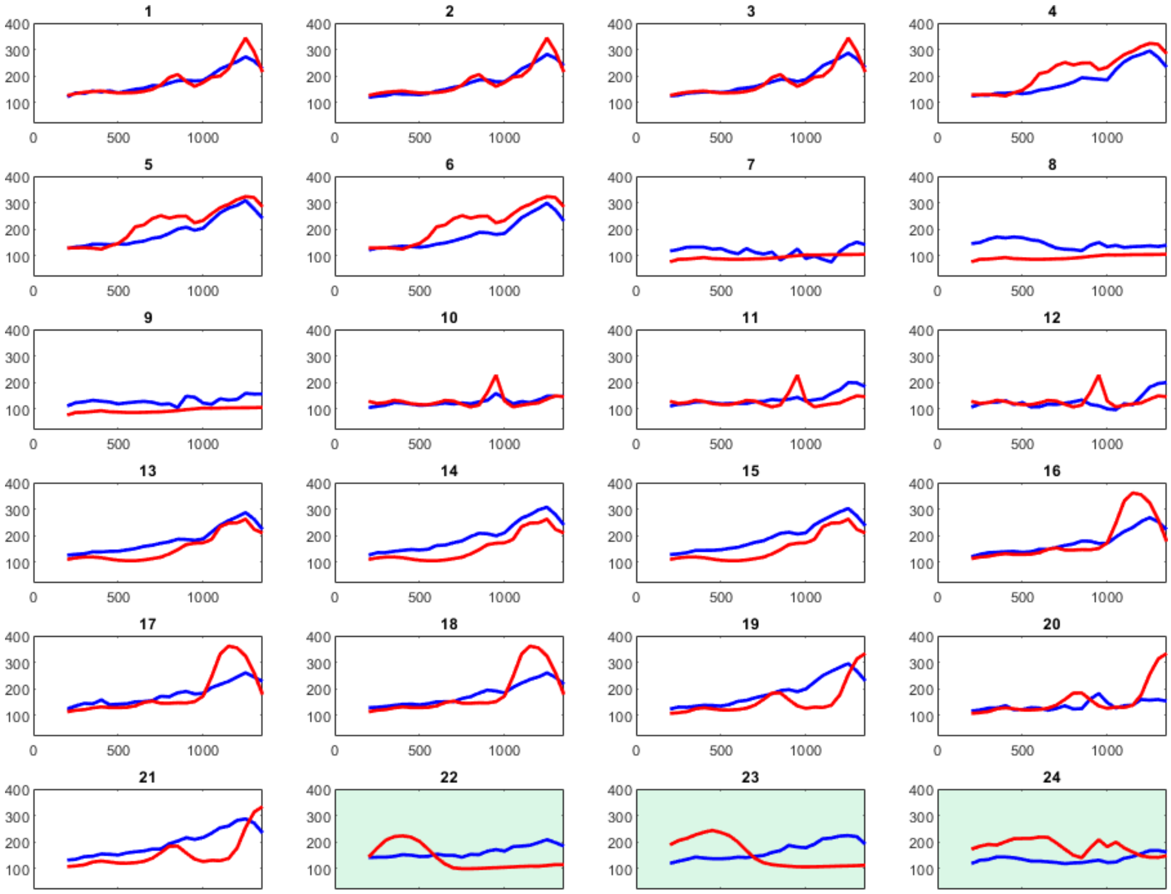

Figure 1: Reconstructed temperature (blue) and TOW measured temperature (Fahrenheit) versus depth (feet) for site A and C. Each location from site A (1 to 21) was trained using 20 modulation-temperature pairs, excluding the location itself. The last 3 plots used all site A data sets for training and used this to predict temperatures for 3 locations at site C, which has different geology.